Functional Roles of ATP-Binding Residues in the Catalytic Site of Human Mitochondrial NAD(P)$^+$-Dependent Malic Enzyme†

Hui-Chih Hung,*,‡ Yu-Ching Chien,‡ Ju-Yi Hsieh,‡ Gu-Gang Chang,§ and Guang-Yaw Liu*,||

Department of Life Sciences, National Chung-Hsing University, Taichung, Taiwan, Faculty of Life Sciences, Institute of Biochemistry, and Structural Biology Program, National Yang-Ming University, Taipei, Taiwan, and Institute of Immunology, Chung-Shan Medical University, Taichung, Taiwan

Received March 21, 2005; Revised Manuscript Received July 22, 2005

ABSTRACT: Human mitochondrial NAD(P)$^+$-dependent malic enzyme is inhibited by ATP. The X-ray crystal structures have revealed that two ATP molecules occupy both the active and exo site of the enzyme, suggesting that ATP might act as an allosteric inhibitor of the enzyme. However, mutagenesis studies and kinetic evidences indicated that the catalytic activity of the enzyme is inhibited by ATP through a competitive inhibition mechanism in the active site and not in the exo site. Three amino acid residues, Arg165, Asn259, and Glu314, which are hydrogen-bonded with NAD$^+$ or ATP, are chosen to characterize their possible roles on the inhibitory effect of ATP for the enzyme. Our kinetic data clearly demonstrate that Arg165 is essential for catalysis. The R165A enzyme had very low enzyme activity, and it was only slightly inhibited by ATP and not activated by fumarate. The values of $K_{m,NAD}$ and $K_{i,ATP}$ to both NAD$^+$ and malate were elevated. Elimination of the guanidino side chain of R165 made the enzyme defective on the binding of NAD$^+$ and ATP, and it caused the charge imbalance in the active site. These effects possibly caused the enzyme to malfunction on its catalytic power. The N259A enzyme was less inhibited by ATP but could be fully activated by fumarate at a similar extent compared with the wild-type enzyme. For the N259A enzyme, the value of $K_{i,ATP}$ to NAD$^+$ but not to malate was elevated, indicating that the hydrogen bonding between ATP and the amide side chain of this residue is important for the binding stability of ATP. Removal of this side chain did not cause any harmful effect on the fumarate-induced activation of the enzyme. The E314A enzyme, however, was severely inhibited by ATP and only slightly activated by fumarate. The values of $K_{m,malate}$, $K_{m,NAD}$, and $K_{i,ATP}$ to both NAD$^+$ and malate for E314A were reduced to about 2−7-folds compared with those of the wild-type enzyme. It can be concluded that mutation of Glu314 to Ala eliminated the repulsive effects between Glu314 and malate, NAD$^+$, or ATP, and thus the binding affinities of malate, NAD$^+$, and ATP in the active site of the enzyme were enhanced.

Malic enzyme catalyzes the divalent metal ion (Mn^{2+} or Mg^{2+}) dependent reversible oxidative decarboxylation of L-malate to yield CO_2 and pyruvate, with concomitant reduction of NAD(P)$^+$ to NAD(P)H (*1*−*5*). The enzymes are widely distributed in nature with conserved sequences and similar overall structural topology among different species (*6*−*9*; see ref *10* for a review). In mammals, according to their nucleotide specificity, three isoforms of malic enzyme have been identified: cytosolic NADP$^+$-dependent (c-NADP-ME;[1] *11*, *12*), mitochondrial NADP$^+$-dependent (m-NADP-ME; *13*), and mitochondrial NAD(P)$^+$-dependent malic enzyme (m-NAD-ME) (*3*, *14*). It has been shown that m-NAD-ME can use both NAD$^+$ and NADP$^+$ as a cofactor, but it favors NAD$^+$ under physiological conditions (*3*). It is believed that human m-NAD-ME, via the NADH and pyruvate products, may play an important role in the metabolism of glutamine in the rapidly proliferating tissues and tumors (*3*, *14*−*21*). The possible involvement of m-NAD-ME in neoplasia makes the enzyme a possible target for the rational drug design in the application of anticancer chemotherapy. In addition to its dual cofactor specificities, m-NAD-ME is distinctive from the other two mammalian isoforms by its complex regulatory system in the control of catalytic activity (*23*, *24*). The m-NAD-ME isoform displays cooperative behavior with respect to the substrate L-malate, and the enzyme activity can be activated by fumarate and inhibited by ATP (*19*, *22*−*27*). Previous kinetic studies have suggested that both fumarate and ATP may operate through an allosteric mechanism (*19*, *23*, *25*), and the allosteric properties of the m-NAD-ME imply its specific role in the pathways of malate and glutamine oxidation in tumor mitochondria (*18*−*23*).

† This work was supported by the National Science Council, ROC (NSC 91-2320-B-005-004 and NSC-93-2311-B-005-018 to H.-C.H.).

* To whom correspondence should be addressed: Telephone: 886-4-2284-0416 (615). Fax: 886-4-22851856. E-mail: hchung@dragon.nchu.edu.tw (H.-C.H.); Telephone: 886-4-2473-0022 (11709). E-mail: liugy@csmu.edu.tw (G.-Y.L.).

‡ National Chung-Hsing University.

§ National Yang-Ming University.

|| Chung-Shan Medical University.

[1] Abbreviations: NAD, nicotinamide adenine dinucleotide; NADH, reduced nicotinamide adenine dinucleotide; NADP, nicotinamide adenine dinucleotide phosphate; NADPH, reduced nicotinamide adenine dinucleotide phosphate; ATP, adenosine triphosphate; c-NADP-ME, cytosolic NADP$^+$-dependent malic enzyme; m-NADP-ME, mitochondrial NADP$^+$-dependent malic enzyme; m-NAD-ME, mitochondrial NAD(P)$^+$-dependent malic enzyme.

10.1021/bi050510b CCC: $30.25
Published on Web 08/31/2005

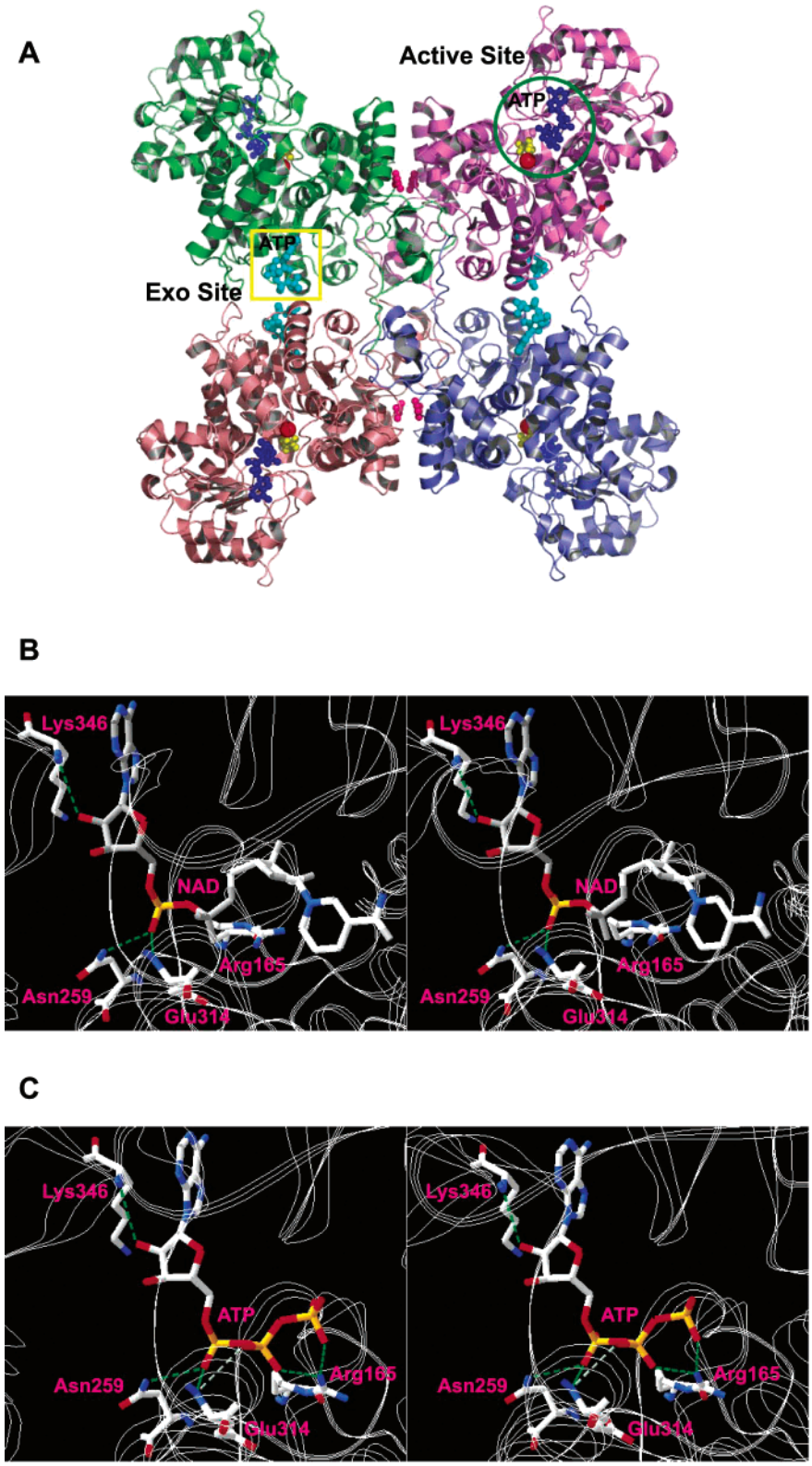

FIGURE 1: Crystal structure and active-site pocket with bound NAD^+ or ATP of the human mitochondrial malic enzyme. (A) Crystal structure of the enzyme in complex with ATP, malate, Mn^{2+}, and fumarate (PDB code 1PJ4). The active- and exo-site regions were highlighted with a green circle and yellow box, respectively; the color is blue for ATP, yellow for malate, and red for Mn^{2+} in the active site, and cyan for ATP in the exo site. This figure was generated with PyMOL (DeLano Scientific LLC, San Carlos, CA). (B and C) NAD- and ATP-binding ligands, respectively, of the human malic enzyme in the active site. The green dashed lines generated by Swiss-Pdb Viewer (*35*) represent the hydrogen bonds between the amino acid residues and NAD^+ or ATP.

The crystal structures of human m-NAD-ME have been reported in open and closed forms (*6*, *7*). Various complex forms with malate/pyruvate, Mn^{2+}/Mg^{2+}, NAD^+, fumarate, and transition-state analogue inhibitors have also been successfully resolved (*28*−*30*). In addition, pigeon c-NADP-ME in a quaternary complex with $NADP^+$, Mn^{2+}, and transition-state analogue oxalate, as well as the *Ascaris suum* m-NAD-ME in an open form and complexed form with

NADH, have also been reported (*8*, *9*, *31*). These structural data establish malic enzymes as a new class of oxidative decarboxylases with a distinct backbone structure (*6*, *10*, *31*).

Malic enzyme is a homotetramer with a dimer of dimers quaternary structure. In the structure of human m-NAD-ME, two NAD^+-binding sites, which are separately located at the active center and an exo site in the tetramer interface, are observed. Furthermore, there is a fumarate-binding site at the dimer interface (Figure 1A) (*29*). The binding of active-site NAD^+ is mainly stabilized by the hydrogen-bonding network that is provided by the nucleotide-binding residues in the active center as shown in Figure 1B. The ATP-binding site has also been determined. The crystal structures of this enzyme in complex with ATP reveal that ATP is bound both in the active and exo sites. The binding mode of ATP in the active site is very similar to that of the active-site NAD^+ (Figure 1C). Kinetic studies have shown that ATP may actually be an active-site inhibitor, rather than an allosteric inhibitor. The inhibition of enzyme activity caused by ATP is due to the competition of ATP with respect to NAD^+ in the active center and not in the exo site (*29*, *32*). The role of ATP in the exo site may be involved in the subunit association of the enzyme (*32*).

In the present paper, we provide detailed kinetic evidences supporting the competitive inhibition between ATP and NAD^+ in the catalytic site of the enzyme. Site-directed mutagenesis is used to explore the functional amino acid residues for ATP inhibition. We chose Arg165, Asn259, and Glu314, which are hydrogen-bonded or ion-paired with active-site NAD^+ and ATP (parts B and C of Figure 1), to identify their significance on the inhibitory effect of ATP. The R165A, N259A, and E314A mutants of malic enzymes have been prepared and kinetically characterized. We describe that the differential effects of these residues in the inhibitory mechanism of ATP is due to its contribution in the hydrogen-bonding network and charge balance with malate, NAD^+, ATP, or other charged residues in the active site of human m-NAD-ME.

EXPERIMENTIAL PROCEDURES

Expression and Purification of Recombinant Malic Enzymes. The detailed expression and purification steps for human m-NAD-ME have been described previously (*3*, *28*), and we modified them from earlier protocols. In brief, the m-NAD-ME was cloned in the expression vector (pRH281) and overexpressed in *E. coli* BL21 cells by controlling of the inducible trp promoter system (*3*). A two-step purification system, an anionic exchange, DEAE-Sepharose (Amersham Biosciences), followed by an ATP-agarose affinity chromatography (Sigma), was used to purify the overexpressed enzyme. After purification, the enzyme was buffer-exchanged and concentrated with a buffer containing 30 mM Tris-HCl (pH 7.4) by Amicon Ultra-15 centrifugal filter devices (Millipore) with a molecular weight cutoff at 30 kDa. The enzyme purity was examined by sodium dodecyl sulfate−polyacrylamide gel electrophoresis (SDS−PAGE), and the protein concentrations were determined by the Bradford method (*33*).

Site-Directed Mutagenesis. Site-directed mutagenesis was carried out using the QuikChange kit (Stratagene). The purified DNA of human m-NAD-ME was used as templates,

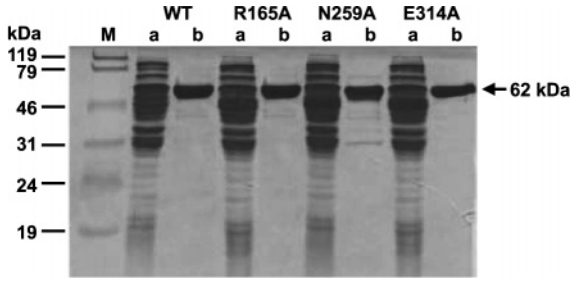

FIGURE 2: Overexpression and purification of the recombinant human mitochondrial malic enzyme. SDS/PAGE was used to examine the expression and purification efficiency. Lane M indicates the molecular-mass markers. Lanes a are those of the crude extract; lanes b are samples from the ATP-agarose column. The arrow indicates the protein band that corresponds to the molecular weight of the monomers of the enzyme.

and the desired primers were used to mutate the Arg165, Asn259, and Glu314 codons to the Ala codon by using *Pfu* DNA polymerase, which replicated both plasmid strands with high fidelity in the PCR reaction. Primers including the mutating site are 25−45-mer, needed for specific binding of template DNA. The synthetic oligonucleotides used as mutagenic primers were 5′-GTAGTGACTGATGGAGAG-**GCT**ATTCTGGGTCTTGGAGATC-3′ for R165A, 5′-CAG-TTCGAAGACTTTGGA**GCT**CATAATGCATTCAGGTTC-3′ for N259A, and 5′-CCTTGGAGCAGGA**GCT**GCTGCTCT-TGGAATTG-3′ for E314A in which the mutation positions are underlined and marked in bold in the oligonucleotide sequence. After 16−18 temperature cycles, mutated plasmids containing staggered nicks were generated. The PCR products were then treated with *Dpn*I to digest the wild-type human m-NAD-ME templates. Finally, the nicked DNA containing desired mutations was transformed into XL-1 *Escherichia coli* strain, and their DNA sequences were checked by autosequencing.

Enzyme Kinetic Analysis. For assay of the m-NAD-ME activity, the reaction mixture contained 50 mM Tris-HCl (pH 7.4), 10 mM malate (pH 7.4), 0.3 mM NAD^+, and 10 mM $MgCl_2$ in a total volume of 1 mL. The absorbance at 340 nm at 30 °C was immediately recorded after the enzyme was added to the reaction mixture and continuously traced in a Beckman DU 7500 spectrophotometer. In this process, 1 unit of the enzyme was defined as the enzyme amount that can catalyze the production of 1 μmol of NADH/min. An absorption coefficient of 6.22 mM^{-1} for NADH was used in the calculations. Apparent Michaelis constants of the substrate and cofactors were determined by varying the concentration of one substrate (or cofactors) around its K_m value, while keeping other components constant at the saturation levels. The inhibition experiment of ATP for malic enzyme activity was carried out at a series of ATP concentrations from 0 to 6 mM in different concentrations of NAD^+ and malate. The whole set of data was analyzed by the following equation describing a competitive inhibition pattern:

$$v = V_{max}/\{1 + K_m/[S]\}/(1 + [ATP]/K_{i,ATP})$$

in which v is the observed initial velocity, V_{max} is the maximum rate of the reaction, K_m is the Michaelis constant for the substrate, and $K_{i,ATP}$ is the inhibition constant for ATP. The inhibition pattern demonstrated in this paper was

Table 1: Kinetic Parameters for the Wild-Type and Active-Site Mutant Human Mitochondrial Malic Enzymes[a]

	$K_{m,malate}$ (mM)	$K_{m,NAD}$ (mM)	$K_{m,Mg}$ (mM)	k_{cat} (s^{-1})
wild type (−)	8.39 ± 1.09	0.35 ± 0.02	1.40 ± 0.11	115.5 ± 3.5
wild type (+)	3.09 ± 0.26	0.23 ± 0.02	0.52 ± 0.04	207.9 ± 2.1
R165A (−)	7.90 ± 0.21	1.67 ± 0.15	1.51 ± 0.10	0.041 ± 0.001
R165A (+)	7.81 ± 0.20	0.60 ± 0.10	0.52 ± 0.02	0.043 ± 0.002
N259A (−)	7.84 ± 0.72	0.42 ± 0.10	0.92 ± 0.10	78.13 ± 1.82
N259A (+)	3.74 ± 0.18	0.29 ± 0.09	0.59 ± 0.06	157.1 ± 3.2
E314A (−)	3.65 ± 0.28	0.05 ± 0.002	1.15 ± 0.05	35.14 ± 0.70
E314A (+)	2.19 ± 0.12	0.03 ± 0.002	0.56 ± 0.03	43.92 ± 0.65

[a] (−) No fumarate added. (+) With 3 mM fumarate added.

presented as the double reciprocal plot. $K_{i,ATP}$ values were calculated with the EZ-FIT program (*34*).

RESULTS

Characterization of the Recombinant Human m-NAD-ME. After a two-step purification, the recombinant malic enzymes were purified to almost homogeneous (Figure 2). The amount of purified protein was 4.9, 16.5, 3, and 6.3 mg from 250 mL of cell lysate, and the specific activity of these enzymes were 48.8, 0.017, 33, 14.8 units/mg for the wild-type, R165A, N259A, and E314A enzymes, respectively. The results indicate that these enzymes were overexpressed at a comparative level and the little specific activity of R165A was due to its enzymatic properties and not the low expression of this mutant.

The kinetic parameters of the recombinant malic enzymes have been determined in the absence or presence of fumarate (Table 1). The k_{cat} value of the R165A mutant was much lower than that of the wild-type enzyme to a level of 2800-fold, indicating that mutation of this residue severely affected the catalytic capability of the enzyme. The $K_{m,NAD}$ value of this mutant was increased by about 3-fold compared with that of the wild-type enzyme, but no obvious change was observed on $K_{m,malate}$ and $K_{m,Mg}$. There were no significant differences on K_m values between the wild-type and N259A enzymes, but the k_{cat} value of N259A was reduced slightly compared with that of the wild-type enzyme. The E314 enzyme, however, had smaller K_m and k_{cat} values compared with that of the wild-type enzyme. The k_{cat} value of this mutant was about one-third of that for the wild-type enzyme, indicating that changing this residue may have a considerable effect on the catalytic power of the enzyme. Furthermore, the K_m values of malate and NAD^+ for this mutant were reduced by 2- and 7-fold, respectively, implying that this mutant increased its affinity for NAD^+ or malate at the active site of the enzyme.

Fumarate could activate the enzyme activity of human m-NAD-ME by decreasing the K_m of substrates and by increasing the k_{cat} of the enzyme. In the presence of 3 mM fumarate, the enzyme activity could be activated by about 2-fold. For the wild-type and N259A enzyme, the kinetic parameters were changed to the similar extents in the presence of fumarate. Their k_{cat} values were raised 1.8−2.0-fold by fumarate, while their K_m values of malate, NAD^+, and Mg^{2+} were reduced by 1.5−3-fold. However, the k_{cat} value of the R165A enzyme was not influenced by fumarate, indicating that this mutant was impaired by its allosteric properties on fumarate activation. The K_m values of NAD^+ and Mg^{2+} for R165A were reduced about 3-fold by fumarate, but little effect on the $K_{m,malate}$ was observed in the presence of fumarate. The E314A enzyme could not be fully stimulated by fumarate. The k_{cat} value was only increased 1.3-fold, while the K_m value of malate was decreased by about 1.7-fold in the presence of fumarate. The K_m values of NAD^+ and Mg^{2+} were reduced about 1.7- and 2.1-fold by fumarate, respectively, similar to those of the wild-type and N259A enzymes.

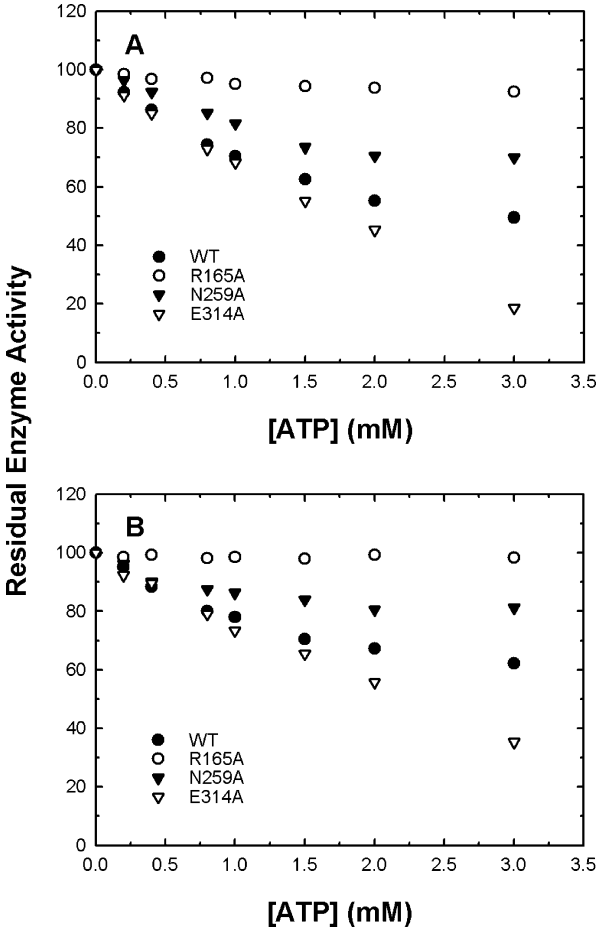

FIGURE 3: Inhibitory effect of ATP on the human mitochondrial malic enzyme. ATP inhibition of the enzyme was assayed in the absence (A) or presence (B) of 3 mM fumarate. Appropriate amount of enzyme was added into the assay mixture containing 10 mM malate, 10 mM $MgCl_2$, and 0.3 mM NAD^+ in 50 mM Tris-HCl (pH 7.4) buffer system in the absence or presence of fumarate. The ATP concentration ranged from 0 to 3 mM.

Inhibitory Effect of ATP on the Wild-Type and Mutant Malic Enzymes. ATP could inhibit the catalytic activity of human m-NAD-ME, whereas fumarate could lessen the inhibition caused by ATP (Figure 3). In the absence of fumarate, the enzyme activity of the wild-type enzyme was gradually inhibited with the increasing concentrations of ATP

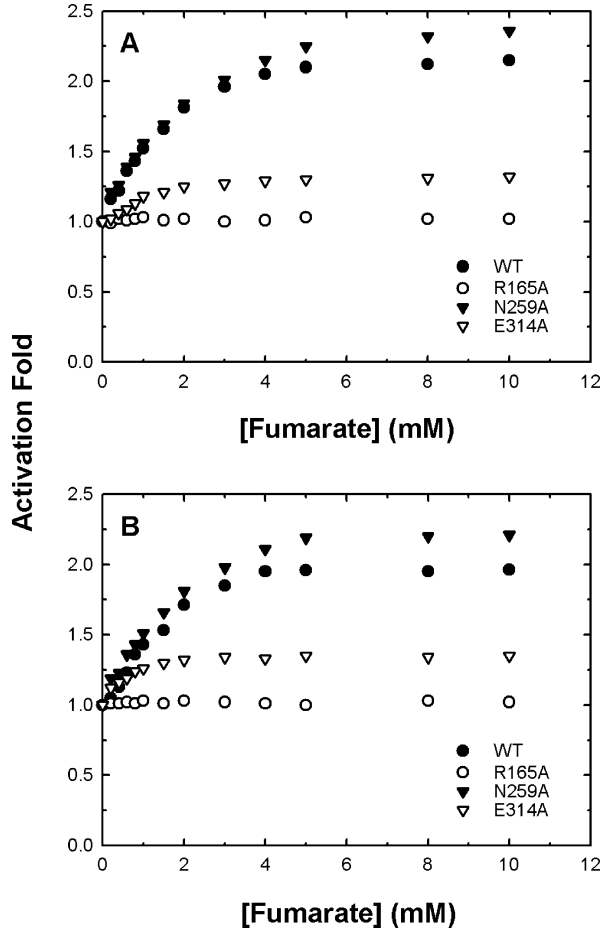

FIGURE 4: Activating effect of fumarate on the inhibited human mitochondrial malic enzyme. The fumarate activation of the enzyme was assayed in the absence (A) or presence (B) of 2 mM ATP. The assay mixture was the same as described in Figure 3 but without or with ATP. The fumarate concentration ranged from 0 to 10 mM.

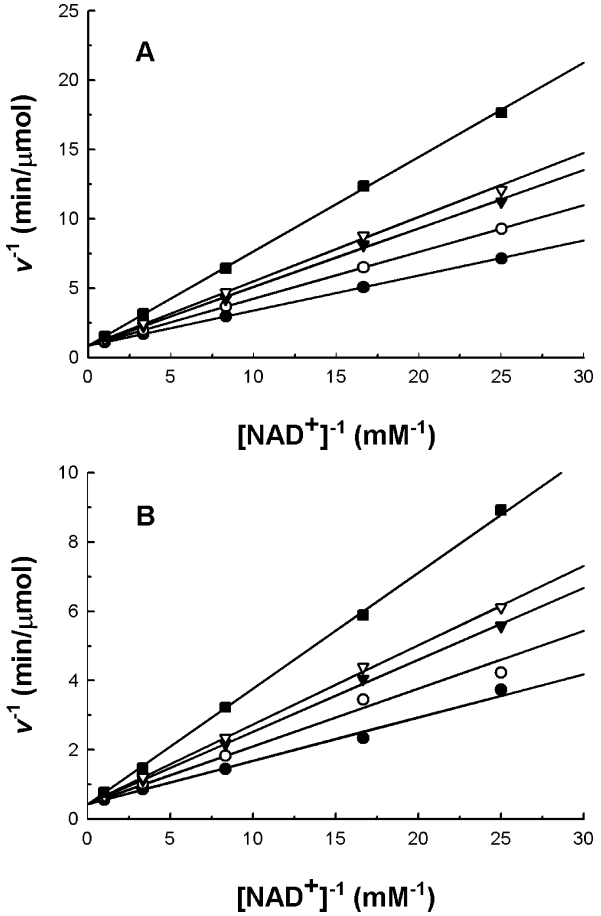

FIGURE 5: Competitive inhibition of the human mitochondrial malic enzyme by ATP with respect to NAD^+. Malic enzyme activity was measured at different concentrations of NAD^+ in various concentrations of ATP. The ATP concentrations used in this experiment, from bottom to top, are 0, 0.4, 0.8, 1, and 2 mM. (A) Without fumarate. (B) With 3 mM fumarate.

and the inhibition steadily reached a plateau, indicating that ATP was saturated in the ATP-binding site (Figure 3A, ●). A similar pattern was observed in the presence of fumarate, but fumarate could reduce the inhibitory effect of ATP on the enzyme (Figure 3B, ●). The residual activities without and with fumarate at 3 mM ATP were 50 and 65%, respectively.

The R165A enzyme only slightly inhibited ATP either in the absence or presence of fumarate (Figure 3, ○). The enzyme activities were almost conserved with increasing ATP concentrations, suggesting that this Arg residue may be crucial for ATP inhibition. ATP had less inhibitory effect on the N259A enzyme. The inhibition curves of this mutant with increasing ATP concentrations were similar to those of the wild-type enzyme, and the inhibition also reached a plateau with the residual enzyme activities remaining above 70 and 80%, respectively, in the absence and presence of fumarate (Figure 3, ▲). Interestingly, to our surprise, the E314 enzyme became more susceptible to ATP inhibition. The residual enzyme activities of this mutant were 20% without fumarate and 40% with fumarate at 3 mM ATP (Figure 3, △).

Activating Effect of Fumarate on the ATP-Inhibitory Malic Enzymes. Fumarate is an allosteric activator for the human m-NAD-ME. In the absence of ATP, the maximal activation achieved by fumarate for the wild-type enzyme was approximately 2.2-fold and that for N259A was 2.4-fold. In the presence of ATP, the activation of these two enzymes reduced slightly about 2-fold (Figure 4, ● for the wild-type enzyme and ▲ for N259A). The E314A enzyme, which is the most sensitive mutant for ATP inhibition (Figure 3, △), could be only activated slightly by fumarate (Figure 4, △). However, for the R165A enzyme without or with ATP, its enzyme activity could not be activated by fumarate (Figure 4, ○); that is, this mutant was insensitive to fumarate.

Competitive Inhibition of the Human m-NAD-ME by ATP. To delineate the inhibitory mechanism of ATP, the malic enzymes were assayed in a broad range of substrates at different fixed concentrations of ATP ranging from 0 to 4 mM (Figure 5 for NAD^+ and Figure 6 for malate as a variable substrate). Our data clearly indicate that the malic enzyme was competitively inhibited by ATP with respect to NAD^+ (Figure 5) or malate (Figure 6). A double-reciprocal plot demonstrated that all lines intercepted at the *y* axis, indicating simple competitive inhibition patterns. The inhibition constant of ATP ($K_{i,ATP}$) with respect to NAD^+ and malate was 1.18 and 1.04 mM, respectively. In the presence of fumarate, the $K_{i,ATP}$ value was slightly elevated (Table 2), indicating that the binding affinity of ATP with the enzyme was reduced by fumarate. Structural studies have revealed that ATP is bound at the NAD-binding site, occupying the adenosine diphosphate-binding region (Figure

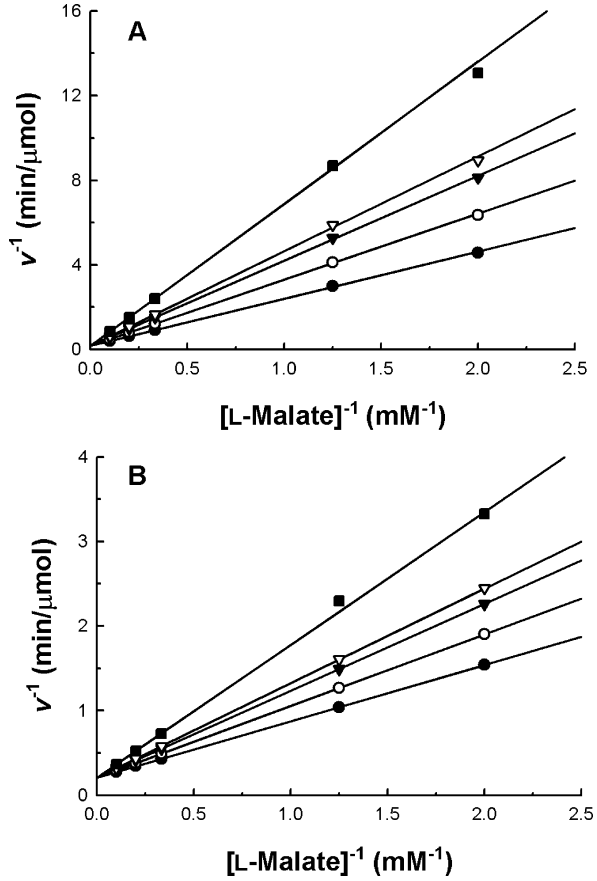

FIGURE 6: Competitive inhibition of the human mitochondrial malic enzyme by ATP with respect to malate. Malic enzyme activity was measured at different concentrations of malate in various concentrations of ATP. The ATP concentrations used in this experiment, from buttom to top, are 0, 0.4, 0.8, 1, and 2 mM. (A) Without fumarate. (B) With 3 mM fumarate.

Table 2: K_i Value for the Wild-Type and Active-Site Mutant Human Mitochondrial Malic Enzymes[a]

	wild type	R165A	N259A	E314A
$K_{i,ATP}$ (mM) (to NAD^+)				
− fumarate	1.18 ± 0.02	5.01 ± 0.96	3.64 ± 0.02	0.51 ± 0.01
+ fumarate	1.92 ± 0.04	8.52 ± 1.02	12.34 ± 0.28	0.75 ± 0.04
$K_{i,ATP}$ (mM) (to malate)				
− fumarate	1.04 ± 0.01	2.25 ± 0.23	1.47 ± 0.01	0.50 ± 0.002
+ fumarate	1.47 ± 0.01	2.17 ± 0.09	1.11 ± 0.003	0.55 ± 0.003

[a] [Fumarate] = 3 mM.

1C). The inhibition thus resulted from the competition of ATP with the nucleotide-binding site in the catalytic center. Furthermore, our data indicate that the $K_{i,ATP}$ value is raised by fumarate, supporting the fact that fumarate could serve as the rescuer, lessening the inhibitory effect of ATP on the enzyme in cells.

The K_i values of these mutants to NAD^+ and malate were shown in Table 2. The R165A mutant had larger $K_{i,ATP}$ values with respect to NAD^+ (5.01 mM) and malate (2.25 mM) than those of the wild-type enzyme. In the presence of fumarate, $K_{i,ATP}$ to NAD^+ was increased (8.52 mM) but $K_{i,ATP}$ to malate was not affected. Similar to R165A, the N259A mutant had a larger $K_{i,ATP}$ value to NAD^+ (3.64 mM), and it was raised to 12.34 mM in the presence of fumarate. On the other hand, the $K_{i,ATP}$ value to malate was close to that of

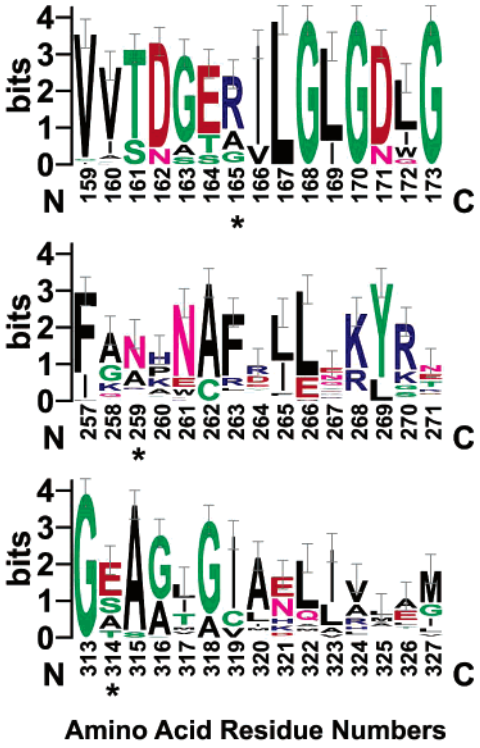

FIGURE 7: Sequence alignments of malic enzymes. Alignments of 35 malic enzymes with amino acid sequences around the NAD^+/ATP-binding region in the active site are shown as sequence logos. Amino acid sequences of malic enzymes were searched by Blast (*36*), and alignments were generated by Clustal W (*37*). The results are represented by sequence logos with error bars (*38*). The amino acid residues highlighted with stars are residues in the NAD^+/ATP-binding region that are mutated in this paper.

the wild-type enzyme and was not affected by fumarate. In contrast to the R165A mutant, the E314A enzyme had smaller $K_{i,ATP}$ to NAD^+ (0.51 mM) and $K_{i,ATP}$ to malate (0.50 mM) than those of the wild-type enzyme, and both of the K_i values were not raised by fumarate.

In summary, the R165A enzyme, with very low enzyme activity, was only slightly inhibited by ATP and was not activated by fumarate. The values of $K_{m,NAD}$ as well as $K_{i,ATP}$ to NAD^+ and malate were raised. ATP has little impact on the catalytic activity of the N259A enzyme. Conversely, this mutant was fully activated by fumarate, similar to the wild-type enzyme. The K_m values of substrates for this mutant did not change. The $K_{i,ATP}$ to NAD^+ but not $K_{i,ATP}$ to malate was elevated. The E314A enzyme, however, became more sensitive to ATP. Its enzyme activity was significantly inhibited by ATP but was not obviously activated by fumarate. The values of $K_{m,malate}$, $K_{m,NAD}$, and $K_{i,ATP}$ of this mutant were reduced to about 2−7-folds compared with those of the wild-type enzyme.

DISCUSSION

Human m-NAD-ME is regulated by ATP as an inhibitor and by fumarate as an activator. The enzyme is believed to participate in the metabolism of glutamine for energy production in fast-growing tissues and tumors. This regulatory machinery operated through ATP and fumarate may be crucial for the functional role of this enzyme, because ATP is the end product of energy metabolism and fumarate is the product of the previous step of the pathway in glutamine metabolism (*21*).

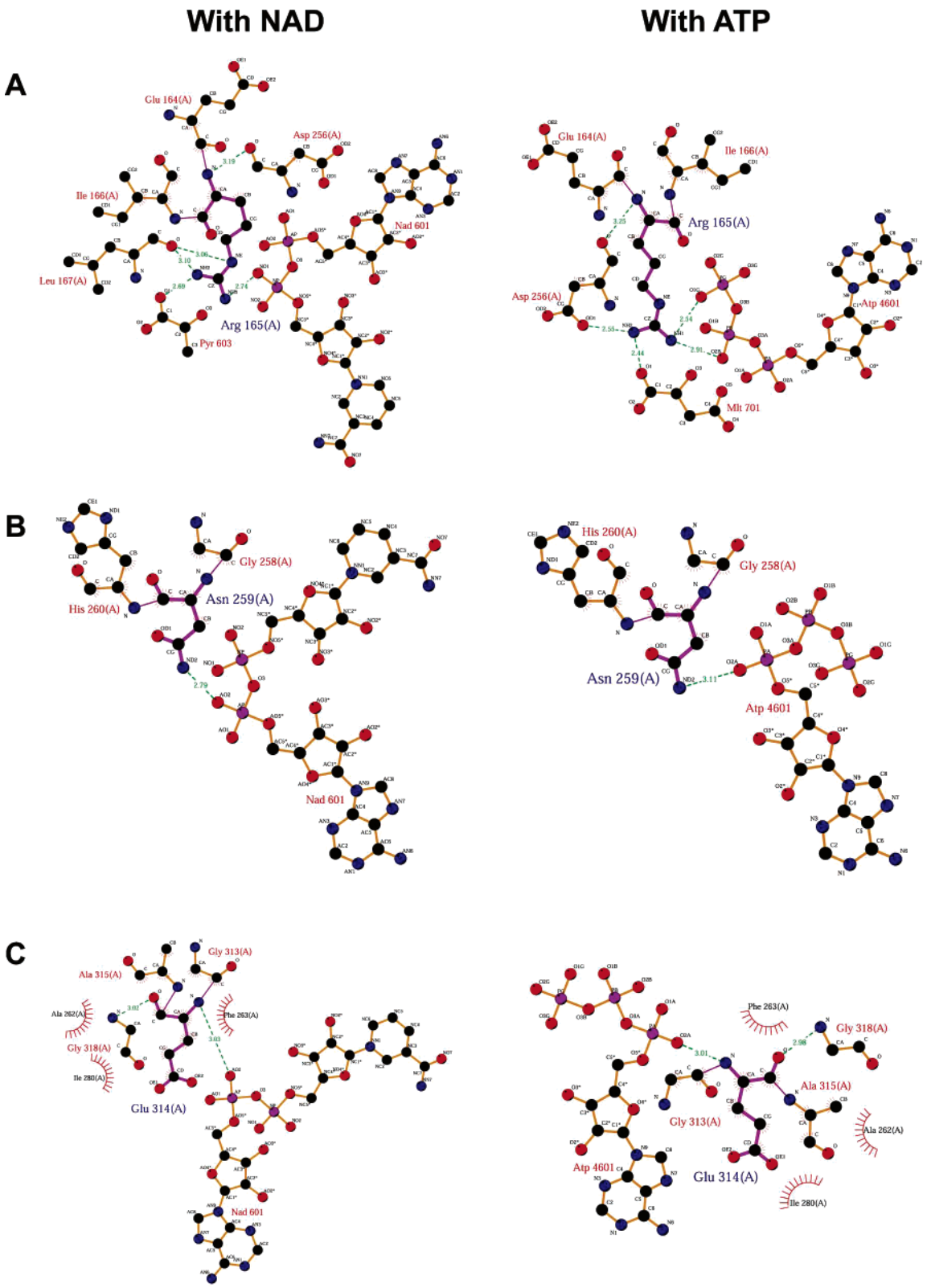

FIGURE 8: LIGPLOT of the NAD- and ATP-binding residues of the human mitochondrial malic enzymes. The ligand interactions are shown as the LIGPLOT diagram (*39*). The bold bonds are the designated amino acid residues, the thin bonds are the hydrogen-bonded residues and NAD or ATP, and the dashed lines represent the hydrogen bonds. Spoked arcs represent hydrophobic contacts.

Structural, mutagenesis, and kinetic studies have suggested that ATP is an active-site inhibitor of the enzyme, despite the other ATP binding in the exo site (*29*, *32*). The exo-site ATP, which is unique to human m-NAD-ME, may be related to the quaternary structural integrity of this enzyme (*32*). In this paper, we explore the functional residues at the active center essential for ATP inhibition. According to the crystal structure of the enzyme with ATP (*29*), we chose Arg165, Asn259, and Glu314, which are hydrogen-bonded or ion-paired with NAD^+ or ATP. They are moderately conserved

in malic enzymes, but they all exist in human isoform enzymes (Figure 7), implying that they may play crucial roles in the active site of the enzyme.

Arg165 Is Essential for Catalysis. In the active site of the enzyme, the binding modes of ATP are similar to those observed in the NAD^+ complex (*29*, *30*). Residues forming the ATP-binding site generally have the same conformations as those in the NAD^+ complex (parts B and C of Figure 1), and there are only small conformational changes for the amino acid residues in the active site. In the active site, Arg165 is ligated to malate/pyruvate and NAD^+/ATP (*29*, *30*). The guanidinium side chain of this residue interacts with the C1 carboxylate group of malate/pyruvate and the phosphates of NAD^+/ATP (Figure 8A). Thus, abolishment of the side chain of R165 may have an effect on the binding of malate, NAD^+, and ATP with the enzyme. Our data demonstrate that a much lower k_{cat} value of R165A than that of the wild-type enzyme as well as an elevated $K_{i,ATP}$ value of about 4-fold was observed. Furthermore, the R165A mutant was only slightly inhibited by ATP and was not allosterically regulated by fumarate. From the structural and kinetic data, we suggest that Arg165 is essentially important for catalysis. Arg165 has a critical role in keeping the active-site structural integrity. Eliminating this side chain causes the enzyme to bind weakly with NAD^+, malate, and ATP, and losing the positive-charged side chain results in charge imbalance in the active site. These effects cause the enzyme to malfunction extensively on its catalytic power.

The enzyme structure with ATP reveals that the side chain of Arg165 has become more disordered, and the conformations of this residue in the four independent monomers are different from each other (*29*). It might reasonably explain the competitive inhibition observed for ATP with respect to malate because ATP and malate are not structurally analogous to each other. Their binding sites in the active center, however, are not distinctively separated because both malate and ATP are ligated with Arg165. After ATP binding to the active site of the enzyme, the side chain of Arg165 becomes more flexible, and this conformation may be unfavorable for malate binding. Thus, the competitive inhibition of ATP with respect to malate is obtained. Nevertheless, a similar inhibition pattern for the R165A mutant is also observed. The loss of a positive charge of Arg165 causes the electrostatic imbalance between malate and ATP (Figure 8A). The additional γ phosphate of ATP may have a sterically charge-repulsive effect that interferes with the binding of malate.

Asn259 Plays an Important Role on ATP Inhibition of Malic Enzyme. Asn259 is a binding ligand for NAD^+ or ATP. The amide side chain of this residue is hydrogen-bonded with NAD^+ or ATP, and the binding networks between Asn259 and NAD^+ or ATP are approximately the same (Figure 8B). Mutation of the amide side chain of Asn259 causes the enzyme to become less sensitive to ATP inhibition, and that may be due to the less binding capability of the mutant enzyme with ATP. Our data reveal that the enzyme activity of the N259A mutant is less inhibited by ATP than that of the wild-type enzyme (Figure 3) and that is corresponded with the raised $K_{i,ATP}$ values to NAD^+ (Table 2). The catalytic efficiency of this mutant, however, is similar to that of the wild-type enzyme, because the k_{cat} and K_m values are not affected by mutation of this residue. Moreover, the N259A mutant could be allosterically activated by fumarate to an extent to that of the wild-type enzyme. Thus, our kinetic studies suggest that the hydrogen-bonding network between Asn259 and ATP is considerably significant for ATP inhibition. Asn259 has a critical role on ATP binding, but this residue is not essential for the binding of NAD^+. Removal of this side chain does not cause the enzyme to malfunction on fumarate activation.

Electrostatic Interaction Is Important for Substrate Binding and Catalysis of Malic Enzyme. The main chain −NH group of Glu314 is hydrogen-bonded with NAD^+ or ATP. The carboxyl side chain of Glu314 does not interact directly with substrates or inhibitors (Figure 8C). Mutation of this residue to alanine supposedly could not cause any significant change in the kinetic properties of the enzyme. Nevertheless, abolishing the negative charge of Glu314 causes the enzyme to have an unexpected impact on ATP inhibition. The E314A mutant was strongly inhibited by ATP (Figure 3). Furthermore, the K_m and K_i values of E314A were reduced, indicating that the binding affinity of substrates and inhibitors with the mutant enzyme was increased (Tables 1 and 2). The catalytic constant of the E314A mutant is about one-third compared with that of the wild-type enzyme. The enzyme activity of this mutant is slightly stimulated by fumarate, but the K_m values were reduced and the K_i values were elevated after the enzyme binds with fumarate, indicating that fumarate still functions on the enzyme. Thus, from the kinetic results and structural information, it could be concluded that the negative charge of Glu314 corresponds to the electrostatic balance that is important in the active site of the enzyme for binding with substrates and inhibitors, as well as catalysis. In the active site of the E314A enzyme, the repulsive effect between the carboxyl side chain of Glu314 and malate, NAD^+, or ATP, all negative-charge rich compounds, has disappeared. Thus, it is reasonable to observe the smaller K_m and K_i values of this mutant.

In this paper, we provide direct kinetic evidence indicating that ATP functions as an active-site inhibitor, rather than an allosteric inhibitor. We also demonstrate that the electrostatic networks in the active site have a significant impact on the binding of the enzyme with malate, NAD^+, and ATP to give a catalytically competent form. The three residues, Arg165, Asn259, and Glu314, however, are also conserved in some other malic enzymes that are not inhibited by ATP (Figure 7) (*24*), suggesting that additional factors govern the binding affinity of ATP in the active site, which might be related to the specific amino acid residues that determine the dual cofactor specificity of the mitochondrial $NAD(P)^+$ malic enzyme.

REFERENCES

1. Frenkel, R. (1975) Regulation and physiological function of malic enzyme, *Curr. Top. Cell. Regul. 9*, 157−181.
2. Hsu, R. Y. (1982) Pigeon liver malic enzyme, *Mol. Cell. Biochem. 43*, 3−26.
3. Loeber, G., Infante, A. A., Maurer-Fogy, I., Krystek, E., and Dworkin, M. B. (1991) Human NAD^+-dependent mitochondrial malic enzyme, *J. Biol. Chem. 266*, 3016−3021.
4. Rao, G. S. J., Coleman, D. E., Kulkarni, G., Goldmith, E. J., Cook, P. F., and Harris, B. G. (2000) NAD-malic enzyme from *Ascaris suum*: Sequence and structural studies, *Protein Pept. Lett. 7*, 297−304.
5. Cleland, W. W. (2000) Chemical mechanism of malic enzyme as determined by isotope effects and alternate substrates, *Protein Pept. Lett. 7*, 305−312.

6. Xu, Y., Bhargava, G., Wu, H., Loeber, G., and Tong, L. (1999) Crystal structure of human mitochondrial NAD(P)$^+$-dependent malic enzyme: A new class of oxidative decarboxylases, *Structure 7*, 877−889.
7. Yang, Z., Floyd, D. L., Loeber, G., and Tong, L. (2000) Structure of a closed form of human malic enzyme and implications for catalytic mechanism, *Nat. Struct. Biol. 7*, 251−257.
8. Yang, Z., Zhang, H., Hung, H. C., Kuo, C. C., Tsai, L. C., Yuan, H. S., Chou, W. Y., Chang, G. G., and Tong, L. (2002) Structural studies of the pigeon cytosolic NADP$^+$-dependent malic enzyme, *Protein Sci. 11*, 332−341.
9. Coleman, D. E., Rao, G. S., Goldsmith, E. J., Cook, P. F., and Harris, B. G. (2002) Crystal structure of the malic enzyme from *Ascaris suum* complexed with nicotinamide adenine dinucleotide at 2.3 Å resolution, *Biochemistry 41*, 6928−6938.
10. Chang, G. G., and Tong, L. (2003) Structure and function of malic enzymes, a new class of oxidative decarboxylases, *Biochemistry 42*, 12721−12733.
11. Loeber, G., Dworkin, M. B., Infante, A., and Ahorn, H. (1994) Characterization of cytosolic malic enzyme in human tumor cells, *FEBS Lett. 344*, 181−186.
12. Chang, G. G., Wang, J. K., Huang, T. M., Lee, H. J., Chou, W. Y., and Meng, C. L. (1991) Purification and characterization of the cytosolic NADP$^+$-dependent malic enzyme from human breast cancer cell line, *Eur. J. Biochem. 202*, 681−688.
13. Loeber, G., Maurer-Fogy, I., and Schwendenwein, R. (1994). Purification, cDNA cloning, and heterologous expression of the human mitochondrial NADP$^+$-dependent malic enzyme, *Biochem. J. 304*, 687−692.
14. Mandella, R. D., and Sauer, L. A. T. (1975) The mitochondrial malic enzymes I. Submitochondrial localization and purification and properties of the NAD(P)$^+$-dependent enzyme from adrenal cortex, *J. Biol. Chem. 250*, 5877−5884.
15. Sauer, L. A., Dauchy, R. T., Nagel, W. O., and Morris, H. P. (1980) Mitochondrial malic enzymes. Mitochondrial NAD(P)$^+$-dependent malic enzyme activity and malate-dependent pyruvate formation are progression-linked in Morris hepatomas, *J. Biol. Chem. 255*, 3844−3848.
16. Baggetto, L. G. (1992) Deviant energetic metabolism of glycolytic cancer cells, *Biochimie 74*, 959−974.
17. Sanz, N., Diez-Fernandez, D., Valverde, A. M., Lorenzo, M., Benito, M., and Cascales, M. (1997) Malic enzyme and glucose 6-phosphate dehydrogenase gene expression increases in rat liver cirrhogenesis, *Br. J. Cancer 75*, 487−492.
18. Moreadith, R. W., and Lehninger, A. L. (1984) The pathways of glutamate and glutamine oxidation by tumor cell mitochondria. Role of mitochondrial NAD(P)$^+$-dependent malic enzyme, *J. Biol. Chem. 259*, 6215−6221.
19. Moreadith, R. W., and Lehninger, A. L. (1984) Purification, kinetic behavior, and regulation of NAD(P)$^+$ malic enzyme of tumor mitochondria, *J. Biol. Chem. 259*, 6222−6227.
20. Fahien, L. A., and Teller, J. K. (1992) Glutamate-malate metabolism in liver mitochondria, *J. Biol. Chem. 267*, 10411−10422.
21. Mckeehan, W. L. (1982) Glycolysis, glutaminolysis, and cell proliferation, *Cell Biol. Int. Rep. 6*, 635−650.
22. Teller, J. K., Fahien, L. A., and Davis, J. W. (1992) Kinetic and regulation of hepatoma mitochondrial NAD(P) malic enzyme, *J. Biol. Chem. 267*, 10423−10432.
23. Sauer, L. A. (1973) An NAD$^+$ and NAD(P)$^+$-dependent malic enzyme with regulatory properties in rat liver and adrenal cortex mitochondrial fractions, *Biochem. Biophys. Res. Commun. 50*, 524−531.
24. Landsperger, W. J., and Harris, B. G. (1976) NAD$^+$-malic enzyme. Regulatory properties of the enzyme from *Ascaris suum*, *J. Biol. Chem. 251*, 3599−3602.
25. Zdnierowicz, S., Swierczynski, J., and Selewski, L. (1988) Purification and properties of the NAD(P)$^+$-dependent malic enzyme from human placental mitochondria, *Biochem. Med. Metab. Biol. 39*, 208−216.
26. Lai, C. J., Harris, B. G., and Cook, P. F. (1992) Mechanism of activation of the NAD-malic enzyme from *Ascaris suum* by fumarate, *Arch. Biochem. Biophys. 299*, 214−219.
27. Karsten, W. E., Pais, J. E., Rao, G. S., Harris, B. G., and Cook, P. F. (2003) *Ascaris suum* NAD-malic enzyme is activated by L-malate and fumarate binding to separate allosteric site, *Biochemistry 42*, 9712−9721.
28. Bhargava, G., Mui, S., Pav, S., Wu, H., Loeber, G., and Tong, L. (1999) Preliminary crystallographic studies of human mitochondrial NAD(P)$^+$-dependent malic enzyme, *J. Struct. Biol. 127*, 72−75.
29. Yang, Z., Lanks, C. W., and Tong, L. (2002) Molecular mechanism for the regulation of human mitochondrial NAD(P)$^+$-dependent malic enzyme by ATP and fumarate, *Structure 10*, 951−960.
30. Tao, X., Yang, Z., and Tong, L. (2003) Crystal structures of substrate complexes of malic enzyme and insights into the catalytic mechanism, *Structure 11*, 1141−1150.
31. Rao, G. S. J., Coleman, D. E., Karsten, W. E., Cook, P. F., and Harris, B. G. (2003) Crystallographic studies on *Ascaris suum* NAD-malic enzyme bound to reduced cofactor and identification of an effector site, *J. Biol. Chem. 278*, 38051−38058.
32. Hsu, W. C., Hung, H. C., Tong, L., and Chang, G. G. (2004) Dual functional roles of ATP in the human mitochondrial malic enzyme, *Biochemistry 43*, 7382−7390.
33. Bradford, M. M. (1976) A rapid and sensitive method for the quantitation of microgram quantities of protein, utilizing the principle of protein-dye binding, *Anal. Biochem. 72*, 248−254.
34. Perrella, F. W. (1988) EZ-FIT: A practical curve-fitting microcomputer program for the analysis of enzyme kinetic data on IBM-PC compatible computers, *Anal. Biochem. 174*, 437−447.
35. Guex, N., and Peitsch, M. C. (1997) SWISS-MODEL and the Swiss-PdbViewer: An environment for comparative protein modeling, *Electrophoresis 18*, 2714−2723.
36. Altschul, S. F., Boguski, M. S., Gish, W., and Wootton, J. C. (1994) Issues in searching molecular sequence databases, *Nat. Genet. 6*, 119−129.
37. Higgins, D., Thompson, J., Gibson, T., Thompson, J. D., Higgins, D. G., and Gibson, T. J. (1994) CLUSTAL W: Improving the sensitivity of progressive multiple sequence alignment through sequence weighting, position-specific gap penalties, and weight matrix choice, *Nucleic Acids Res. 22*, 4673−4680.
38. Crooks, G. E., Hon, G., Chandonia, J. M., and Brenner, S. E. (2004) WebLogo: A sequence logo generator, *Genome Res. 14*, 1188−1190.
39. Wallace, A. C., Laskowski, R. A., and Thornton, J. M. (1995) LIGPLOT: A program to generate schematic diagrams of protein−ligand interactions, *Protein Eng. 8*, 127−134.

BI050510B